

Influence of Departures from LTE on Determinations of the Sulfur Abundances in A–K Type Stars

S. A. Korotin¹ and K. O. Kiselev¹

Crimean Astrophysical Observatory, Nauchny, Crimea, Russia
e-mail: serkor1@mail.ru

Received date; accepted: date

ABSTRACT

The influence of departures from local thermodynamic equilibrium (LTE) on neutral sulfur lines is considered. A grid of corrections is proposed to take into account the influence of departures from LTE for neutral sulfur lines in the visible and infrared spectral regions, including the H-band. The grid is calculated using the atomic model of sulfur incorporating the most up-to-date collision rates with electrons and hydrogen. The inclusion of levels and transitions of ionized sulfur in the atomic model made it possible to expand the range of effective temperatures of stellar photospheres in the grid up to 10000 K. The atomic model was tested in determining the sulfur abundance of 13 stars and showed its adequacy in a wide range of fundamental stellar parameters. In the spectra of all test stars, the sulfur lines are fitted with similar abundances of the element, regardless of the degree of influence of the effects of deviation from LTE on a particular spectral line. For lines of several multiplets, the wavelengths and oscillator strengths were refined. A list of S I lines recommended for determining sulfur abundance has been created.

Key words. line formation, line profiles of stars, elemental abundances on the Sun

1. INTRODUCTION

To understand the processes of chemical evolution in the Galaxy and the history of star formation, researchers examine the relationships between various chemical elements in stellar atmospheres. Iron-peak elements and α -elements play a fundamental role in these studies, as their nucleosynthesis occurs over different timescales. α -Elements can be used as cosmic clocks to monitor both stellar nucleosynthesis and the history of galaxy formation. Unlike other α -elements, sulfur is moderately volatile. For this reason, its abundance measured in stars within the Local Group galaxies can be directly compared to its abundance measured in extragalactic H II regions. While α -elements are produced by Type II supernovae, iron-peak elements are produced by Type Ia supernovae over longer timescales. Among the various α -elements, the nucleosynthesis of sulfur is not fully understood. Sulfur is formed during the final stages of evolution of massive stars ($M > 20 M_{\odot}$). Hydrostatic burning of neon in the core at temperature of 1.2×10^9 K leads to the formation of a convective oxygen core and the production of α -elements, including sulfur. Further, various nuclear transformation processes occur, resulting in the near-total destruction of the produced sulfur during the Si-burning phase. However, sulfur production continues with oxygen burning in the outer layers around the core, as well as through explosive oxygen burning during Type II supernova explosions (Limongi & Chieffi 2003; Kobayashi et al. 2020). This enrichment is assumed to occur over a relatively short timescale on the order of tens of millions of years. Accordingly, it can be expected that the [S/Fe] ratio will be relatively constant for low-metallicity stars. These are stars that formed before the ignition of the first Type Ia supernovae. This ratio then decreases as iron levels increase. There is still no consensus on whether this “plateau” exists in the relative sulfur abundance of metal-deficient stars. The authors of Israelian & Rebolo

(2001) suggested that the [S/Fe] ratio continues to increase at [Fe/H] < 2.0. Other studies ((Spite et al. (2011), Kacharov et al. (2015), and others) have shown evidence of a plateau, although this plateau has significant dispersion due to the complicated analysis of weak lines at such low metallicities. In stars with near-solar heavy element abundance, sulfur behaves as a typical α -element. Within the range of $-1 < [\text{Fe}/\text{H}] < 0$, the [S/Fe] ratio decreases to zero, which confirms the general characteristics of α -element nucleosynthesis.

However, sulfur has received little attention from researchers. Analysis of sulfur is often omitted in favor of other α -elements, whose measurements are less complex. The issues at hand include the weakness of sulfur’s optical lines. In the optical range, there are 6, 8, and 10 multiplets with relatively weak lines that nearly vanish in metal-deficient stars. Two triplets in the near-infrared region, λ 9212–9237 and λ 10455–10459 Å are heavily affected by departures from local thermodynamic equilibrium (LTE) (Takeda et al. (2005), Korotin (2009)). These lines are located in a region of the spectrum that is significantly distorted by lines from Earth’s atmosphere. For these reasons, studies of sulfur are often bypassed in favor of simpler analyses of other α -elements. As a result, our understanding of sulfur’s behavior is still insufficient compared to other α -elements.

The influence of non-LTE effects on sulfur lines requires detailed study. As shown in Takeda et al. (2005) and Korotin (2009), non-LTE corrections for S I lines have complex dependences on the fundamental parameters of stars and the sulfur abundance itself. Model calculations Takeda et al. (2005) and Korotin (2009) show similar patterns in the behavior of non-LTE corrections depending on stellar parameters, though the corrections differ slightly in magnitude. It should be noted that since these model calculations were conducted, new atomic data have become available for neutral and ionized sulfur. The use of new

detailed quantum-mechanical calculations of inelastic collision rates with electrons and hydrogen should help avoid potential errors introduced by approximate formulas. We have worked on updating the sulfur atomic model Korotin (2009), incorporating the latest atomic data and verifying it with spectra of well-studied stars.

2. SULFUR ATOM MODEL

Our previously developed sulfur atom model (Korotin 2009) included 64 levels of neutral sulfur and the ground level of S II. Approximate formulas were used to account for collisional interactions with electrons and hydrogen, though they were often of limited accuracy. Over time, our knowledge of the atomic parameters of sulfur has significantly improved. Detailed quantum-mechanical calculations have occurred for collisional rates of inelastic interactions between 56 levels of neutral sulfur and hydrogen (Belyaev & Voronov 2020). Previously, the collisions with hydrogen in the atomic model were accounted for using the so-called ‘‘Drawin formula’’ (Drawin 1968; Steenbock & Holweger 1984). It is well known that this formula gives highly inaccurate results, which researchers attempted to correct by introducing empirical correction factors, obtained by adjusting non-LTE calculations to observations. Comparisons between this approximate formula and the detailed calculations (Belyaev & Voronov 2020) show discrepancies that can reach several orders of magnitude. A similar situation exists for collisional rates with electrons. The ADAS database (Summers & O’Mullane 2011) now includes detailed calculations for collisional interactions of the 17 lowest levels of sulfur with free electrons, allowing us to abandon the use of inaccurate approximate formulas. Moreover, applying the old atomic model to study sulfur lines in A-type stars with sufficiently high effective temperatures raised the need to include additional levels of S II and S III in the model. All this prompted us to upgrade the atomic model and perform the appropriate testing.

As in the previous model, the populations of 64 energy levels of neutral sulfur were considered in detail. The highest S I level in the model is separated from the continuum by 0.21 eV, which ensures reliable interaction at temperatures above 2500 K. Additionally, 81 levels of S II and the ground level of S III were included. The highest S II level is separated from the continuum by 0.45 eV, corresponding to a temperature of 5150 K. To more fully account for particle numbers, we included one level of S I, six levels of S III, and the ground level of S VI, with populations calculated in LTE. Fine structure levels were not considered. The values of electronic energy levels were taken from Martin et al. (1990). The diagram of the sulfur atom levels is shown in Fig. 1.

Detailed consideration included 775 bound-bound and 146 bound-free transitions between levels. Line profiles were calculated using the Voigt profile, taking into account radiative broadening as well as Stark and Van der Waals broadening. The number of points along the profile varied from 30 to 110, depending on the line’s intensity. Photoionization cross sections and oscillator strengths were taken from the TOPBase database (Cunto et al. 1993). For forbidden transitions, oscillator strengths were obtained from the catalog Hirata & Horaguchi (1994).

Detailed quantum-mechanical calculations of collisional excitation rates by electrons for transitions among 17 levels of neutral sulfur were obtained from the ADAS database (Summers & O’Mullane 2011). For transitions among the 32 lower levels of ionized sulfur, we used calculations from Tayal & Zatsarinny (2010). For other allowed transitions, we ap-

plied the formula from van Regemorter (1962), and for forbidden transitions, the formula from Allen (1973), with an effective collision strength set to 1. Collisional ionization was accounted for using the formula from Seaton (1962) with the photoionization threshold cross-section from TOPBase (Cunto et al. 1993).

Collisional interactions with hydrogen atoms become very important in the atmospheres of stars with low effective temperatures and metal-poor stars, where electron density decreases. Although the actual collisional rates with hydrogen are quite small, the high concentration of hydrogen provides a significant influence on the redistribution of electronic level populations. Recently, detailed quantum-mechanical calculations for inelastic collisions between various atoms and hydrogen have made it possible to account for this effect more realistically than with approximate approaches. For the sulfur atom, such calculations were performed in (Belyaev & Voronov 2020). We incorporated collisional interactions with hydrogen for forty levels of neutral sulfur within a temperature range of 1000 to 10000 K. Beyond this range, extrapolation was applied; however, the effect of collisional interactions with hydrogen becomes negligible at such high temperatures.

To obtain the sulfur level populations in stellar atmospheres, we used the MULTI software package (Carlsson 1986), version 2.3, which we modified slightly (Korotin et al. 1999). The main changes involve using the complete opacity calculation package from the ATLAS9 software (Castelli & Kurucz 2003), including the so-called opacity distribution function (ODF) arrays. After solving the statistical equilibrium and radiative transfer equations together, we obtained coefficients of deviation from LTE populations, known as b-factors: the ratio of non-LTE to LTE populations ($N_{\text{NLTE}}/N_{\text{LTE}}$). These were passed to the synthetic spectrum calculation software SynthV (Tsymbal et al. 2019), where sulfur line profiles were calculated with non-LTE effects, while lines of other elements were calculated under the LTE approach. Line parameters necessary for synthetic spectrum calculations were taken from the VALD database (Ryabchikova et al. 2015).

3. APPLICATION OF THE SULFUR ATOM MODEL TO SOLAR SPECTRUM ANALYSIS. REFINEMENT OF NEUTRAL SULFUR LINE PARAMETERS

After updating the sulfur atom model, it is necessary to validate its accuracy. This requires comparing the model with observed spectra from several stars with well-known atmospheric parameters. These stars’ atmospheric parameters should span a broad range of temperatures and pressures. Validation of the model is performed by comparing observed and synthetic profiles of spectral lines that belong to different multiplets and exhibit different degrees of deviation from values predicted in the LTE approximation. For instance, some spectral lines show no considerable non-LTE effects, while others display significant deviations from LTE. Such a combination of lines cannot be accurately modeled in an LTE approach by simply adjusting the element’s abundance. A well-selected atomic model in non-LTE calculations should allow an acceptable description of this spectrum using a consistent element abundance for all analyzed lines.

Only a limited number of S I lines are suitable for determining sulfur abundance in the visible spectrum. These include the first (λ 9212–9237 Å), sixth (λ 8694 Å), eighth (λ 6743–6757 Å), and tenth (λ 6046–6052 Å) quintet system multiplets. In the near-infrared range, multiplet lines at λ 10455–10459 Å, λ 15400–15422 Å, λ 15469–15478 Å and λ 22507–22707 Å. The remain-

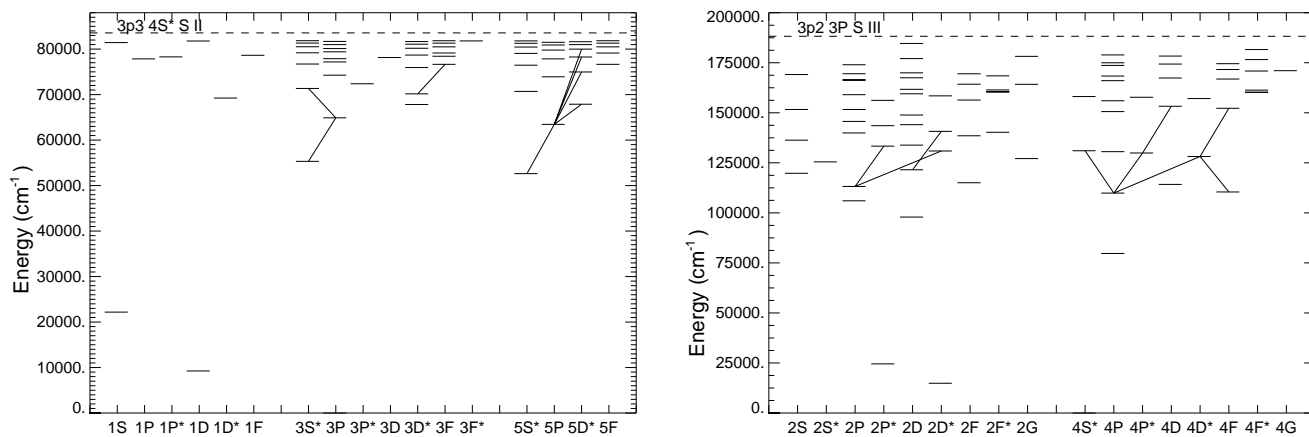


Fig. 1. Grotrian diagrams for S I (left) and S II (right). Only transitions used to determine sulfur abundances are shown.

ing lines are either too weak or blended. Notably, the eighth and tenth multiplets each consist of three lines, and each line itself is a superposition of three components with slight wavelength shifts. Such line profiles deviate significantly from a Gaussian shape, necessitating synthetic spectrum calculations for comparison with observations, as illustrated in the figures below. Using equivalent widths for these lines requires caution and the application of methods for calculating equivalent widths of multicomponent lines.

For analyzing neutral sulfur lines, we used the solar spectrum from atlases Kurucz et al. (1984) and Reiners et al. (2016), covering the range from λ 3000 to λ 13000 Å and λ 4050 to λ 23000 Å, respectively. Calculations were based on a solar atmosphere model Castelli & Kurucz (2003) with a microturbulent velocity of 1 km/s. The Sun’s rotational velocity was set at 1.8 km/s. Element abundances in the solar atmosphere were taken from Asplund et al. (2021). Profiles of all lines included Van der Waals broadening, calculated according to Barklem & O’Mara (1997); Barklem et al. (1998).

Calculations of neutral sulfur level populations for the solar photosphere showed results consistent with Korotin (2009). The sixth, eighth, and tenth multiplet lines form almost in LTE and are not influenced by non-LTE effects. The lines in the IR H-range behave similarly. Only the lines of two IR triplets, λ 9212–9237 and λ 10455–10459 Å are significantly enhanced due to overpopulation of their lower levels, $4s\ 5S^*$ and $4s\ 3S^*$, and underpopulation of their upper levels, $4p\ 5P$ and $4p\ 3P$, respectively, at the line formation depths. The b-factor distribution of some sulfur levels by photospheric depth is shown on the left panel of Fig. 2. The population levels between which the sixth, eighth, and tenth multiplet transitions form are in LTE at these line formation depths. The right panel of Fig. 2 shows the ratio of the source function S_l to the Planck function B_ν for both IR triplets as a function of optical depth. It is evident that at the line formation depths, $S_l/B_\nu < 1$. Thus, non-LTE effects strengthen the lines, leading to negative corrections to sulfur abundance estimates when using the LTE approach for these multiplet lines.

Experimentally, oscillator strengths and wavelengths have only been determined for the triplet lines at λ 10455–10459 Å (Zerne et al. 1997). For other sulfur lines, only theoretical calculations are available, notably in Biemont et al. (1993) (hereafter BQZ). More recent results are presented in Zatsarinny & Bartschat (2006) (hereafter ZB). Studies Froese Fischer et al. (2006) (hereafter FTI) and Deb & Hibbert

(2008) (hereafter DH) cover only part of the S I lines examined here.

Oscillator strengths for the lines of the first multiplet are nearly identical in ZB, FTI, and DH, with differences not exceeding 0.03 dex and an estimated accuracy of 25%. For further calculations, we used data from ZB for these lines.

Figure 3 compares the calculated line profiles of two IR triplets, including non-LTE effects, with the observed solar spectrum. All lines except for λ 9212 Å, which is distorted by Earth’s atmosphere, are described well at a sulfur abundance $(S/H) = 7.16$, with a profile fitting error of no more than ± 0.02 dex. The non-LTE correction for the lines of the first IR triplet (λ 9212–9237 Å) is -0.23 dex, while for the λ 10456 Å line, the non-LTE correction is -0.18 dex. This derived sulfur abundance aligns with the sulfur abundance in chondrites: $(S/H) = 7.15 \pm 0.02$ (Lodders 2021). The sulfur abundance in these meteorites is determined with high accuracy and can be used as a reference for the Solar System. Given that the Sun is a main-sequence dwarf star, its photosphere likely retains its original composition, so the sulfur abundance should match the meteoritic value. Agreement between the IR triplet-derived sulfur abundance and meteoritic levels can serve as a confirmation of the adequacy of our sulfur atom model.

The analysis of other sulfur lines in the optical range showed that using wavelengths and oscillator strengths from the VALD (Ryabchikova et al. 2015) or NIST (Kramida et al. 2012) databases to calculate the synthetic spectrum did not yield ideal line profiles. This is understandable, since the oscillator strength calculation accuracy varies from 25 to 40% depending on the source. For example, for the sixth multiplet lines, the log gf values from ZB and BQZ differ by 0.31 dex. Wavelengths are also calculated based on electronic level energies, which are typically determined with an accuracy of ± 25 – 30 cm^{-1} (Martin et al. 1990). Given that optical-range S I lines are unaffected by non-LTE effects, we refined their wavelengths and oscillator strengths. This procedure of refinement of line parameters serves for finding a balance between observational data and theoretical values of wavelengths and oscillator strengths.

The sixth multiplet is the triplet at λ 8693–8694 Å. The log gf values of this triplet from BQZ are systematically lower than ZB by 0.31 dex and lower than DH by 0.45 dex. Profiles calculated using BQZ oscillator strengths were much weaker than observed. ZB values produced a more realistic synthetic spectrum, though profiles were still slightly weaker than observed. At the

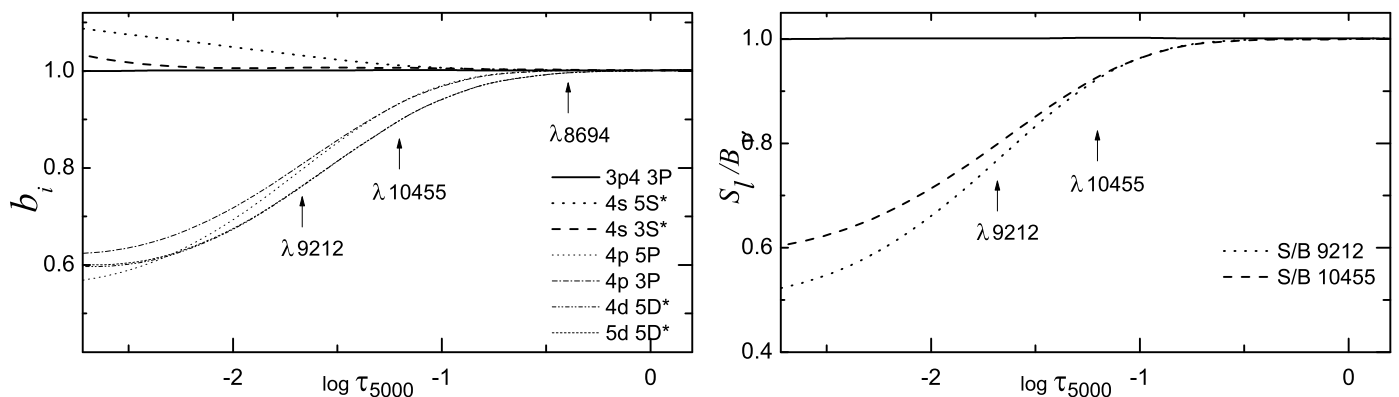


Fig. 2. Distribution of b-factors in the Sun's atmosphere (left panel) and the variation of the S_I/B_V ratio with depth for two IR triplets (right panel). Arrows indicate the formation depths of some sulfur lines

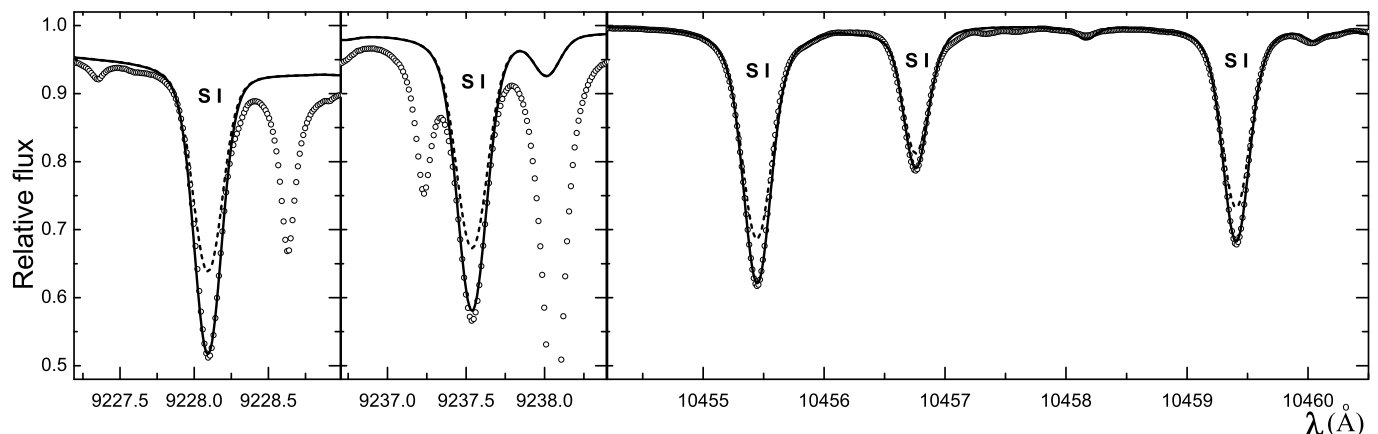


Fig. 3. Comparison of observed (circles) and synthetic profiles of IR triplet lines in the Sun's spectrum. The non-LTE profile for sulfur abundance (S/H) = 7.16 is shown as a solid line, and the LTE profile, calculated with the same abundance, is shown as a dashed line.

same time, oscillator strengths from DH resulted in excessively strong calculated lines. The difference between $\log gf$ from DH and ZB is 0.13 dex for all components of the multiplet. The best agreement between synthetic and observed profiles was achieved with values of $\log gf_{ZB} + 0.088$. We also adjusted the multiplet component wavelengths. The shift does not exceed 0.07 Å from those in VALD, which is within the stated accuracy range.

The eighth multiplet is the triplet at $\lambda 6743$ - 6757 Å. Each component in this triplet is itself a triplet of closely spaced lines. The $\log gf$ values of these nine lines from BQZ are on average lower than ZB by 0.11 dex. DH calculations for this multiplet are unavailable. When using BQZ oscillator strengths with meteoritic sulfur abundance, the theoretical lines are weaker than observed, while ZB data produced slightly stronger lines than observed. The best agreement is achieved at $\log \log gf_{ZB} + 0.075$, which is close to the BQZ values, but slightly lower. It should be noted that the wavelengths of these multiplet components vary by up to 0.1 Å across different sources. The multiplet itself is a combination of transitions between three lower and five upper levels. Lower level energies are relatively well-determined, particularly for the upper levels of the first multiplet lines at $\lambda 9212$ - 9237 Å. By varying upper level energies, we attempted to achieve the best description of the observed profiles. Energy corrections did not exceed 25 cm^{-1} . The maximum wavelength shift relative to VALD recommendations was 0.06 Å, which is consistent with various discrepancies from the literature.

The tenth multiplet is the triplet at $\lambda 6041$ - 6052 Å. Each component in this triplet is also a triplet of closely spaced lines. The $\lambda 6041$ Å line is blended with a strong iron line and was excluded from analysis. DH and BQZ do not provide calculations for this multiplet, and VALD values are on average lower than ZB by 0.15 dex. Profiles calculated with these oscillator strengths were weaker than observed. A satisfactory description for the $\lambda 6052$ Å line was achieved by increasing $\log gf_{ZB}$ by 0.113 dex for all components in this triplet. We also adjusted the wavelengths of two line components, with a maximum shift of 0.03 Å. However, this oscillator strength adjustment did not provide a good fit for the $\lambda 6046$ Å line in the observed spectrum. This line is clearly broadened by an unknown component in the solar spectrum. Thus, we excluded this line from further analysis.

Figure 4 presents examples of synthetic profiles with refined parameters, describing the observed solar spectrum. The refined line parameters are listed in Table 1.

4. COMPARISON OF NON-LTE CALCULATIONS WITH OBSERVED STELLAR SPECTRA

4.1. Late-Type Stars

After refining the SI line parameters based on the solar spectrum, we tested the sulfur atom model against spectra of late-type stars. We selected well-studied stars with reliably deter-

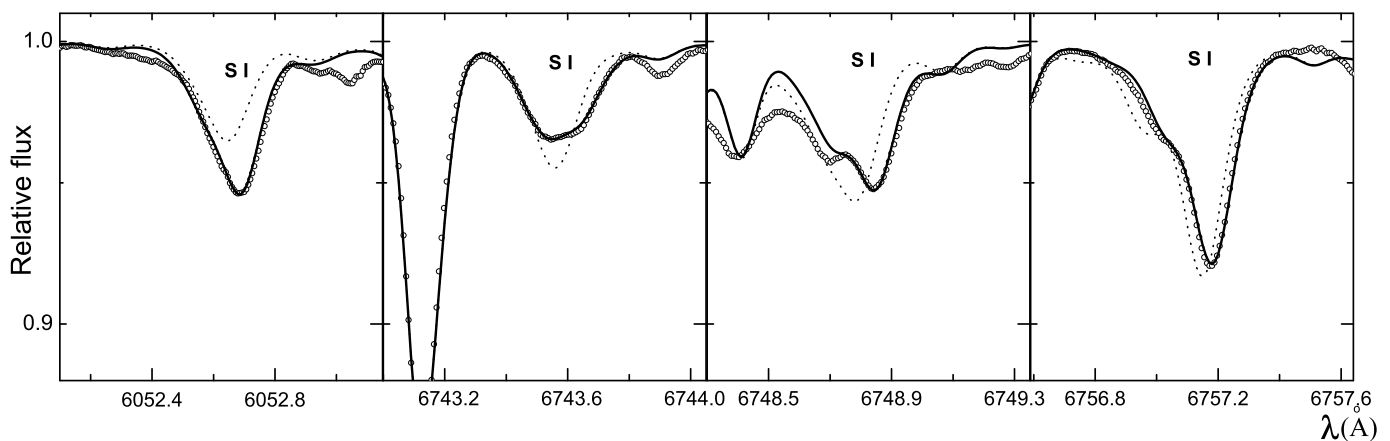


Fig. 4. Comparison of observed (circles) and synthetic profiles of the eighth and tenth multiplet lines in the Sun's spectrum. Profiles with refined parameters are shown as solid lines, and those calculated with VALD parameters are shown as dotted lines.

Table 1. Parameters of S I lines

$\lambda, \text{\AA}$	E, eV	$\log gf$	Γ_{vw}	$\lambda, \text{\AA}$	E, eV	$\log gf$	Γ_{vw}
6052.53	7.87	-1.99	-6.55	10455.45	6.86	0.25	-7.32
6052.59	7.87	-1.15	-6.55	10456.76	6.86	-0.45	-7.32
6052.69	7.87	-0.56	-6.55	10459.41	6.86	0.03	-7.32
6743.47	7.87	-1.24	-6.65	15400.08	8.70	0.43	-7.00
6743.54	7.87	-0.88	-6.65	15403.72	8.70	-0.30	-7.00
6743.65	7.87	-0.94	-6.65	15403.79	8.70	0.61	-7.00
6748.61	7.87	-1.36	-6.65	15422.20	8.70	-1.84	-7.00
6748.71	7.87	-0.77	-6.65	15422.26	8.70	-0.30	-7.00
6748.85	7.87	-0.56	-6.65	15422.28	8.70	0.77	-7.00
6756.86	7.87	-1.71	-6.65	15469.82	8.05	-0.17	-6.90
6757.03	7.87	-0.86	-6.65	15478.48	8.05	0.06	-6.90
6757.18	7.87	-0.28	-6.65	22507.56	7.87	-0.48	-7.44
8693.16	7.87	-1.29	-6.98	22519.07	7.87	-0.25	-7.44
8693.95	7.87	-0.45	-6.98	22552.57	7.87	-0.04	-7.44
8694.64	7.87	0.14	-6.98	22563.83	7.87	-0.26	-7.44
9212.87	6.53	0.39	-7.37	22575.39	7.87	-0.73	-7.44
9228.09	6.53	0.25	-7.37	22644.06	7.87	-0.34	-7.44
9237.54	6.53	0.02	-7.37	22707.74	7.87	0.44	-7.44

mined fundamental parameters. For an accurate atomic model, lines from various multiplets should be described by close sulfur abundances across a broad range of stellar atmospheric parameters. The study included the following stars. Three stars with solar-like composition: hot dwarf Procyon, hot giant HD 195295, and cool giant Pollux. Two metal-poor stars: Ceti and HD 22879, as well as the metal-deficient star HD 84937. Thus, the stars used in the analysis differ greatly from each other. The stars were selected with low rotation velocities to minimize profile distortion.

Fundamental parameters were taken from Jofré et al. (2015) for all stars except HD 195295, for which data were taken from Lyubimkov et al. (2010). The spectrum for HD 195295 was obtained using the 2.7-m telescope spectrograph at McDonald Observatory (Tull et al. 1995) with a resolution $R = 60\,000$. The spectra of the remaining objects, obtained with the UVES spectrograph at the Paranal Observatory (Tull et al. 1995), were taken from the ESO archive. They all have a spectral resolution of at least 75 000 and a signal-to-noise ratio of at least 200. The spectra were processed and the continuum was drawn using the Dech package (Galazutdinov 2022). The atmosphere models of the stars were calculated using the ATLAS9 software with the ODF from Mészáros et al. (2012). The parameters of the stars are given in Table 2. It also contains the results of determining the sulfur abundance for the multiplets used in the analysis (one line for each multiplet) and the corresponding non-LTE correc-

tions. The abundances obtained from the lines within the multiplet are nearly identical. The given error in the average abundance, reflecting the line-to-line scatter, shows a very small variation. The real error in determining the element's abundance will be slightly higher, since it should include the effect of the inaccuracy of the fundamental parameters of the star.

The IR triplet at λ 10455–10459 Å, unfortunately, could only be used for Procyon, Pollux, and HD 195295, since other spectra either had excessive noise in this range or did not cover it. For Pollux and τ Ceti, the λ 6052 Å line was heavily blended with CN molecular lines, and it was very weak for HD 84937, so it was excluded from analysis. Lines of the eighth multiplet were also nearly invisible in HD 84937, with equivalent widths below 1 mÅ. However, there is a clear depression at the λ 6757 Å line, which aligns well with the sulfur abundance determined from the first and sixth multiplet lines. This serves as an additional support for the derived sulfur abundance. Figure 5 shows examples comparing synthetic and observed profiles. It can be seen that, despite the varying sensitivity of lines from different multiplets to non-LTE effects depending on stellar atmospheric parameters, they yield closely aligned sulfur abundances. This can be considered as a good confirmation of the adequacy of the atomic model used in our analysis.

4.2. Sulfur Lines in A-Type Stars

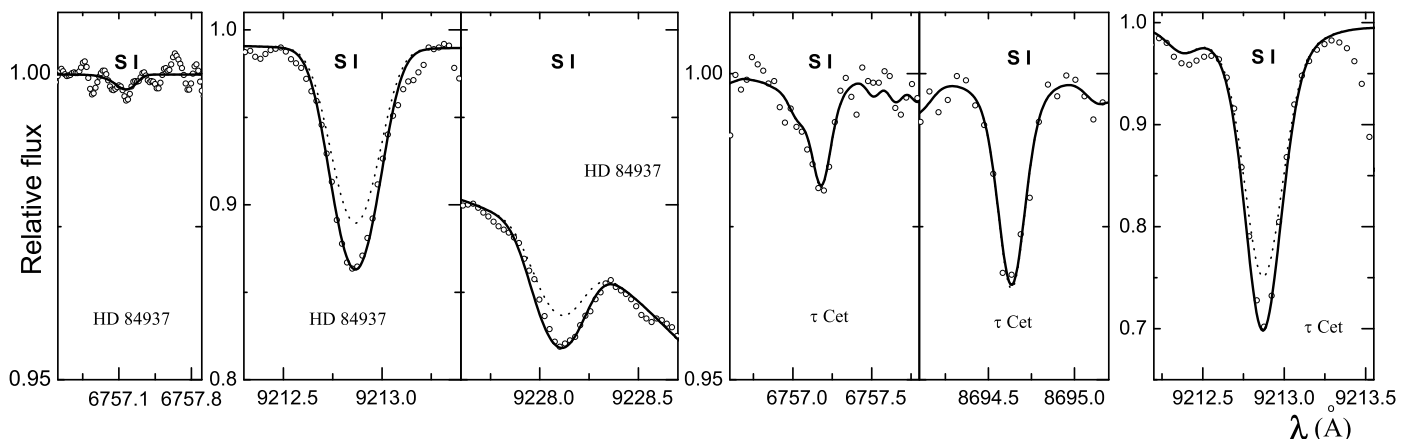
The next step in validating our model involved applying it to hotter stars whose spectra feature sulfur in both S I and S II lines. These are A-type stars with temperatures above 9500 K, where ionized sulfur lines become visible while neutral sulfur lines in the visible spectrum also remain relatively intense. For this analysis, we selected two stars, ρ Peg and θ Vir, studied in Romanovskaya et al. (2023). These stars have temperatures of 9600 K and $\log g = 3.8$ and 3.6, respectively. The spectra were acquired using the ESPaDOnS spectrograph (Petit et al. 2014) at a resolution $R = 68\,000$. For ρ Peg, a procedure of averaging 12 spectrograms was performed, which allowed the signal-to-noise ratio to be increased to 700. Details are given in Romanovskaya et al. (2023).

The parameters of the ionized sulfur lines used for the analysis are given in Table 3. The oscillator strengths are taken from Irimia & Froese Fischer (2005). All lines are weak, from 2 to 7 mÅ, but are well detected due to the high quality of the spectra. These lines form deep in the photosphere and are therefore

Table 2. Sulfur abundance in the stars

Star	Stellar parameters					Sulfur abundance (S/H)					NI
	T_{eff}	$\log g$	[Fe/H]	V_t	$V \sin i$	6052	6757	8694	9212	10455	
Procyon	6554	3.99	0.01	1.66	2.8	7.10	7.11	7.15	7.13	7.13	12
HD195295	6570	2.32	0.00	3.60	8.0	7.02	7.07	7.06	7.08	7.08	10
Pollux	4858	2.90	0.13	1.28	2.0		7.20	7.25	7.15	7.10	6
τ Ceti	5414	4.49	-0.49	0.89	0.4		6.74	6.67	6.67		6
HD 22879	5868	4.27	-0.86	1.05	4.4	6.56	6.56	6.53	6.50		6
HD 84937	6356	4.15	-2.03	1.39	5.2		5.40	5.36	5.34		5
ρ Peg	9597	3.80	0.25	1.98	5.4	7.48	7.53	7.56	7.62	7.52	11
θ Vir	9600	3.60	0.15	1.42	0.5	7.40	7.46	7.44	7.44		7
HD 24040	5809	4.12	0.09	1.00	1.5	7.23	7.21	7.19	7.17	7.20	12
HD 28005	5802	4.18	0.21	1.00	3.5	7.34	7.35	7.34	7.36	7.36	10
HD 34445	5803	4.06	-0.03	1.00	4.5	7.23	7.25	7.22	7.18	7.18	12
HD 82943	5917	4.23	0.13	1.00	4.0	7.32	7.34	7.32	7.32	7.32	9
HD 87359	5645	4.40	-0.07	1.00	4.0	7.14	7.18	7.14	7.14	7.16	10

	Average (S/H)		Non-LTE corrections, dex				
	Opt. range	H-range	6052	6757	8694	9212	10455
Procyon	7.12 ± 0.02		-0.02	-0.02	-0.06	-0.48	-0.51
HD195295	7.08 ± 0.04		-0.06	-0.08	-0.21	-0.81	-0.83
Pollux	7.17 ± 0.05			0.00	-0.02	-0.30	-0.18
τ Ceti	6.71 ± 0.04			0.00	0.00	-0.13	
HD 22879	6.54 ± 0.02		0.00	0.01	0.00	-0.19	
HD 84937	5.35 ± 0.03			0.00	0.00	-0.14	
ρ Peg	7.55 ± 0.05		-0.03	-0.04	-0.07	-0.37	-0.34
θ Vir	7.43 ± 0.03		-0.02	-0.03	-0.06	-0.35	
HD 24040	7.19 ± 0.02	7.26 ± 0.04	0.00	0.00	0.00	-0.20	-0.15
HD 28005	7.35 ± 0.01	7.32 ± 0.03	0.00	0.00	0.00	-0.21	-0.15
HD 34445	7.21 ± 0.02	7.23 ± 0.03	0.00	0.00	0.00	-0.22	-0.16
HD 82943	7.32 ± 0.01	7.30 ± 0.03	0.00	0.00	-0.01	-0.22	-0.15
HD 87359	7.16 ± 0.02	7.15 ± 0.01	0.00	0.00	0.00	-0.17	-0.11

**Fig. 5.** Comparison of observed (circles) and synthetic profiles of neutral sulfur lines in the spectra of HD 84937 and t Cet. The non-LTE profile is shown as a solid line, while the LTE profile, calculated with the same abundance, is shown as a dashed line.

nearly free from the influence of non-LTE effects, which lead to a very small (by several percent) enhancement. Figure 6 shows examples of comparison of theoretical and observed sulfur line profiles in two degrees of ionization.

Non-LTE results for neutral sulfur lines in the analyzed A-type stars are summarized in Table 2. For the S II lines, non-LTE sulfur abundances $(S/H) = 7.51 \pm 0.04$ and 7.38 ± 0.04 were obtained for ρ Peg and θ Vir, respectively. These values show a difference of only 0.04 dex from the average sulfur abundance derived from S I lines. This is smaller than the uncertainties that may arise from oscillator strengths and fundamental stellar pa-

rameters. Thus, we conclude that the sulfur atom model is applicable up to effective temperatures of 10000 K.

5. NEUTRAL SULFUR LINES IN THE INFRARED H-RANGE

Recently, spectral studies in the H-range have expanded. The emergence of high-resolution IR spectrographs, such as GI-ANO (Origlia et al. 2014), has significantly enhanced the capability to determine the chemical composition of stellar atmo-

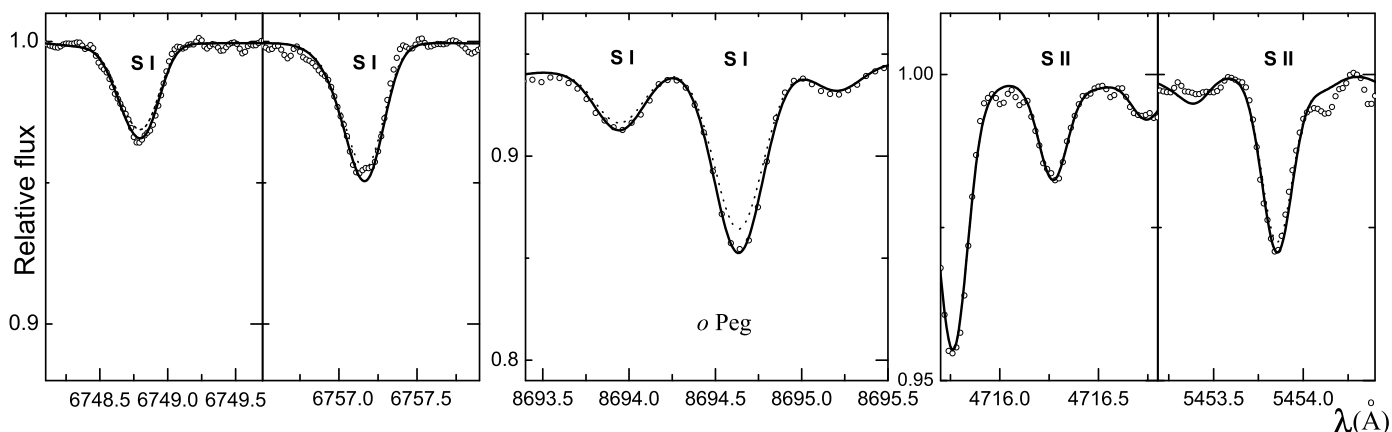


Fig. 6. Comparison of observed (circles) and synthetic profiles of neutral and ionized sulfur lines in the spectrum of *o* Peg. The non-LTE profile is shown as a solid line, and the LTE profile, calculated with the same abundance, is shown as a dashed line.

Table 3. Parameters of S II lines

λ (Å)	E_{low}	$\log gf$	λ (Å)	E_{low}	$\log gf$
4162.665	15.944	0.780	5014.042	14.067	0.046
4294.402	16.135	0.560	5032.434	13.671	0.188
4716.271	13.617	-0.365	5428.655	13.584	-0.177
4815.552	13.671	0.068	5453.855	13.671	0.442
4925.343	13.584	-0.206	5606.151	13.733	0.124
5009.567	13.617	-0.234	5639.977	14.067	0.258

spheres. This includes determining sulfur abundance based on lines from three infrared multiplets: λ 15400–15422, λ 15469–15478 and λ 22507–22707 Å. In Korotin et al. (2020), some analysis of the non-LTE effects on these lines was performed using the 2009 sulfur model. The lines of two multiplets in the region of λ 15400 Å show minimal sensitivity to deviations from LTE, while the remaining lines form almost in LTE in the atmospheres of solar-type dwarfs. These conclusions remained unchanged with the use of a new atomic model.

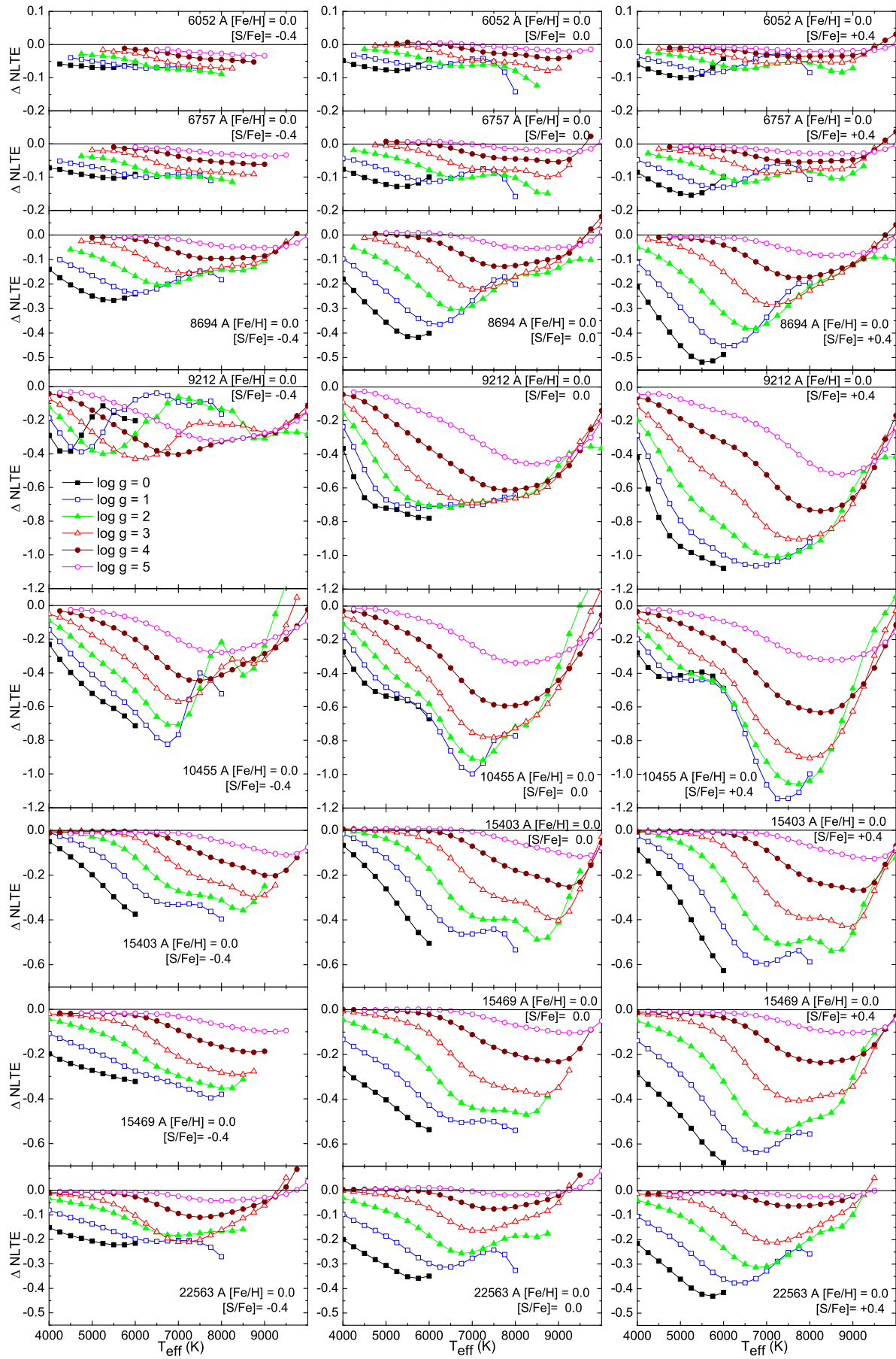
For testing, we used five stars from Korotin et al. (2020), which have IR spectra obtained with the GIANO spectrograph, as well as optical spectra from the ESO archive obtained with the UVES spectrograph. This allows a comparison of sulfur abundances determined from sulfur lines in the optical and H ranges. The parameters of the stars are given in Table 2. The parameters of the S I lines used in the H-range are shown in Table 1. The oscillator strengths for lines of the two multiplets in the region of λ 15400 Å from BQZ and ZB have a systematic difference of 0.16 to 0.19 dex. As discussed in detail in Korotin et al. (2020), observed profiles for the Sun and the studied stars are better described when using the value $\log gf = BQZ - 0.12$ dex. For the λ 22507–22707 Å lines, the BQZ and ZB oscillator strengths differ randomly, yielding similar average abundances. The calculations used BQZ data. The results in Table 2 show that the abundances obtained from lines in the optical range agree reasonably well with those from the H-range.

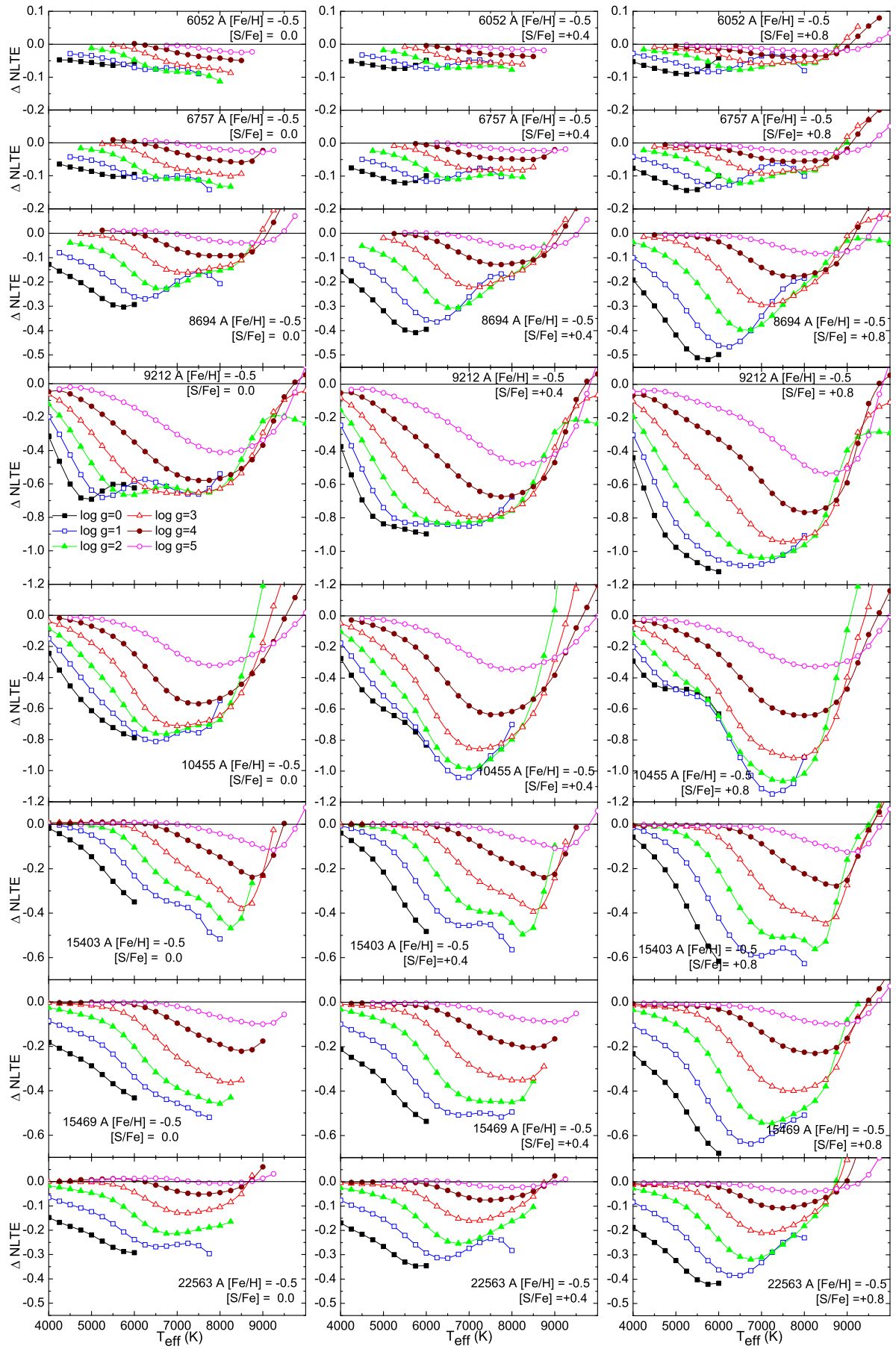
6. NON-LTE CORRECTION GRID FOR NEUTRAL SULFUR LINES

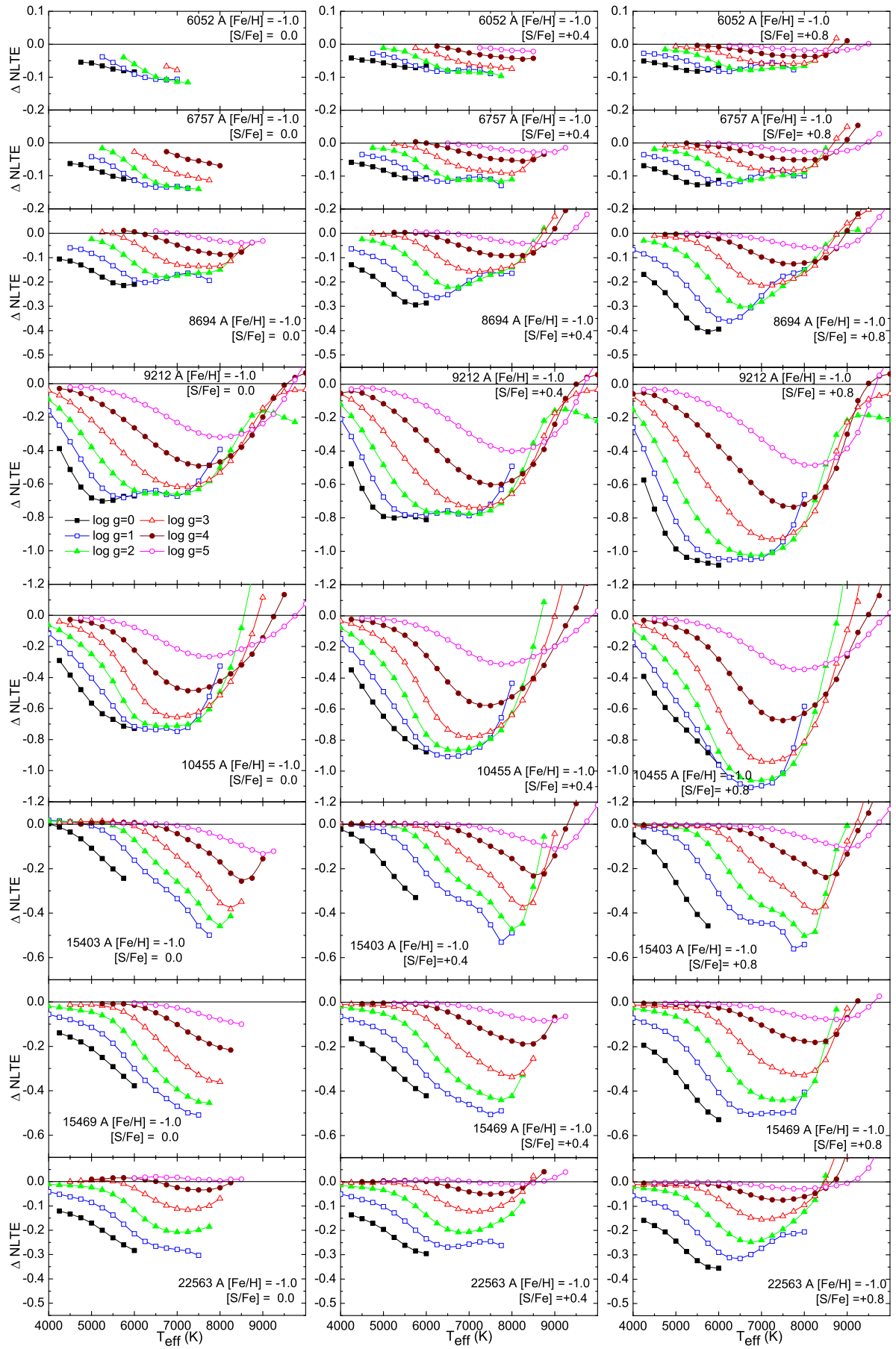
After verifying the atomic model and refining the parameters of S I lines suitable for sulfur abundance determination, we calculated a grid of non-LTE corrections. Unlike the studies

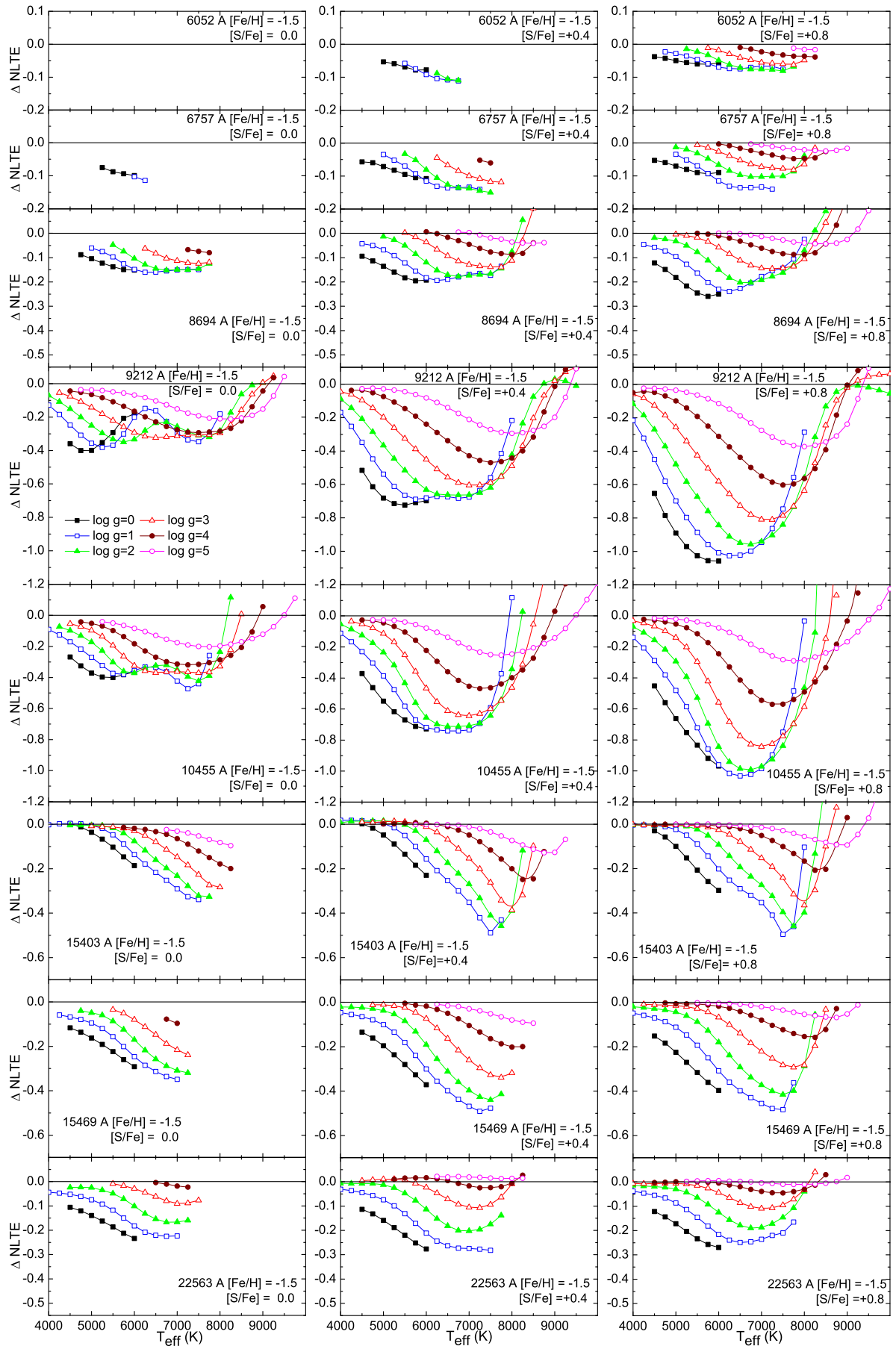
Takeda et al. (2005) and Korotin (2009), this grid includes lines in the H-range and extends to higher effective temperatures. The range of stellar atmosphere parameters spans effective temperatures from 4000 to 10000 K, acceleration of gravity $\log g$ from 0 to 5 and heavy element abundance $[Fe/H]$ from 0 to -2 . The microturbulent velocity was chosen to be 2 km/s. Calculations for solar metallicity atmospheres were performed with sulfur abundances $[S/Fe] = -0.4; 0.0; +0.4$ dex, while for metal-poor models, the values were $[S/Fe] = 0.0; +0.4; +0.8$ dex, since such stars usually exhibit excesses of α -elements. Calculations were performed by adjusting the sulfur abundance so that the equivalent width with non-LTE effects, matched the LTE value at the corresponding grid point. The difference between these abundances represents the correction due to non-LTE effects. Corrections were not calculated for lines with an equivalent width less than 5 mÅ. It should be noted that the magnitude of non-LTE corrections can be significantly affected by microturbulent velocity, since it can considerably alter the line formation depth for strong lines. The calculation results are presented in the form of graphs (Figs. 7–11) since they visually illustrate and allow better assessment of the degree of non-LTE effects for each star, compared to the tables. Some general trends can be observed. As expected, the absolute value of corrections increases from dwarfs to giants, as the less dense atmosphere of giants reduces the impact of collisional processes that promote thermodynamic equilibrium. Lines of the eighth (λ 6743–6757 Å) and tenth (λ 6046–6052 Å) multiplets in dwarfs have the smallest corrections and can be used in LTE analysis. Non-LTE effects on these lines are significant only for giants. The same conclusion applies to all lines in the H-range. Lines of the sixth (λ 8694 Å) multiplet are slightly more sensitive to LTE deviations, while lines from the two IR triplets can only be used if non-LTE corrections are applied. The non-LTE correction grid is available in electronic form. An example of these data is provided in Table 4, where the first column lists the wavelength, followed by $[Fe/H]$, $[S/Fe]$, and T_{eff} , with non-LTE corrections for five $\log g$ values in subsequent columns.

In general, the absolute value of corrections initially increases with effective temperature, since the UV radiation field actively affects the redistribution of sulfur level populations. However, upon reaching a maximum around 7000–8000 K, the corrections start to decrease as more sulfur atoms become ionized, sulfur lines weaken, and form deeper in the star’s atmosphere where collisional processes become more influential. For stars with effective temperatures above 9500 K, non-LTE cor-

Fig. 7. Non-LTE corrections for metallicity $[\text{Fe}/\text{H}] = 0$


 Fig. 8. Same as Fig. 7 for $[\text{Fe}/\text{H}] = -0.5$

Fig. 9. Same as Fig.7 for $[\text{Fe}/\text{H}] = -1.0$


 Fig. 10. Same as Fig.7 for $[\text{Fe}/\text{H}] = -1.5$

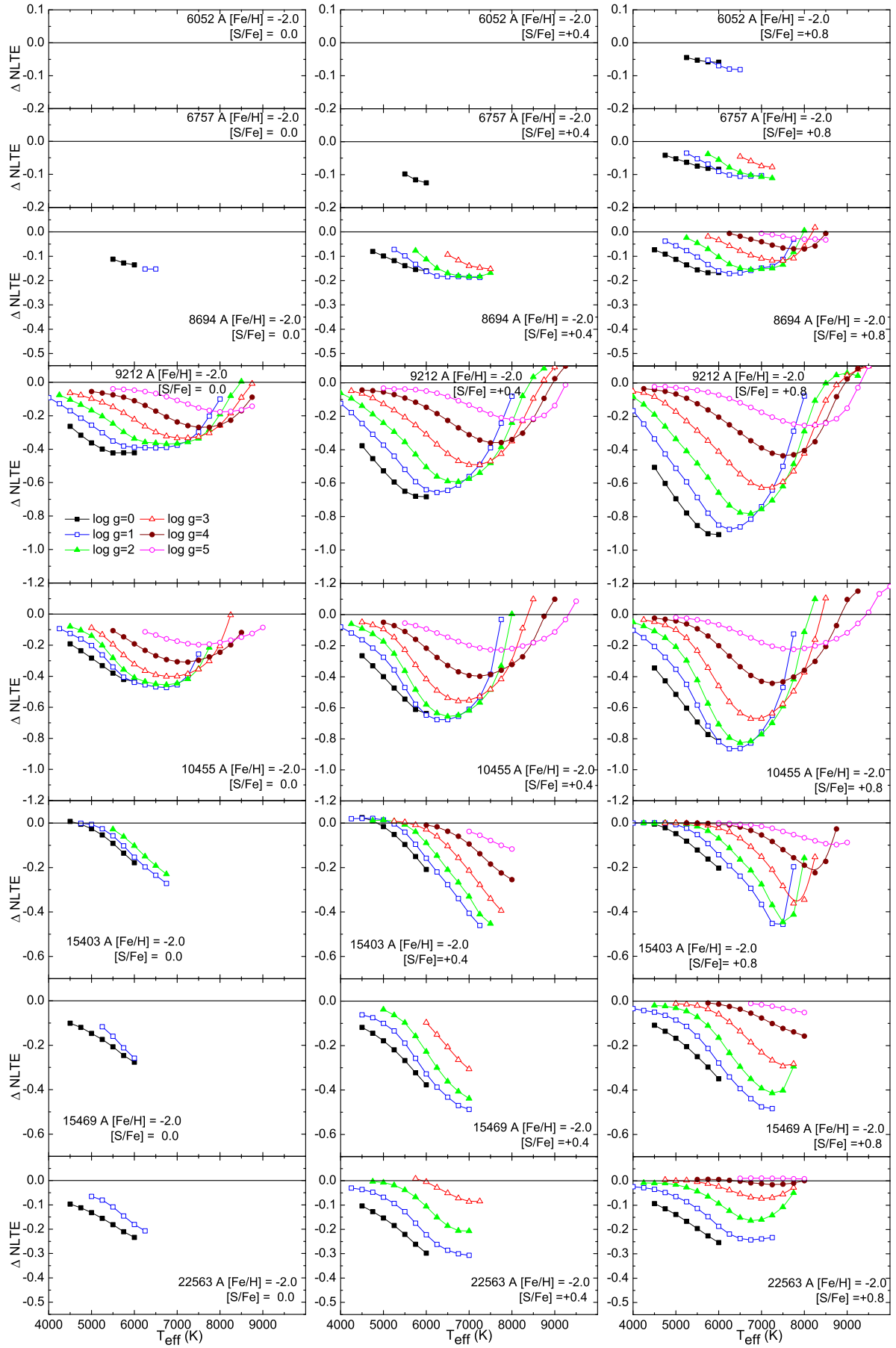


Fig. 11. Same as Fig.7 for $[\text{Fe}/\text{H}] = -2.0$

Table 4. Grid of non-LTE corrections for S I lines

λ , Å	[Fe/H]	[S/Fe]	T_{eff}	log g=0	log g=1	log g=2	log g=3	log g=4	log g=5
6052.7	0.0	-0.4	4000						
6052.7	0.0	-0.4	4250	-0.06					
6052.7	0.0	-0.4	4500	-0.06	-0.04				
6052.7	0.0	-0.4	4750	-0.06	-0.04	-0.03			
6052.7	0.0	-0.4	5000	-0.07	-0.05	-0.03			
6052.7	0.0	-0.4	5250	-0.07	-0.05	-0.03	-0.02		
6052.7	0.0	-0.4	5500	-0.07	-0.06	-0.04	-0.02		
6052.7	0.0	-0.4	5750	-0.06	-0.07	-0.04	-0.02	-0.01	
6052.7	0.0	-0.4	6000	-0.06	-0.07	-0.05	-0.03	-0.01	
6052.7	0.0	-0.4	6250		-0.07	-0.06	-0.03	-0.02	
6052.7	0.0	-0.4	6500		-0.07	-0.07	-0.04	-0.02	-0.02
6052.7	0.0	-0.4	6750		-0.07	-0.07	-0.05	-0.03	-0.01
6052.7	0.0	-0.4	7000		-0.07	-0.08	-0.06	-0.03	-0.02
6052.7	0.0	-0.4	7250		-0.07	-0.08	-0.06	-0.04	-0.02
6052.7	0.0	-0.4	7500		-0.08	-0.08	-0.07	-0.04	-0.02
6052.7	0.0	-0.4	7750			-0.08	-0.07	-0.04	-0.03
6052.7	0.0	-0.4	8000			-0.09	-0.07	-0.05	-0.03
6052.7	0.0	-0.4	8250				-0.07	-0.05	-0.03
...

rections for most lines in dwarf stars become minimal or may even change sign. However, sulfur lines in such stars also become very weak. The correction value is also highly dependent on sulfur abundance, as it affects the intensity of sulfur spectral lines and, consequently, the depth at which they form.

Applying non-LTE corrections to determine abundances is generally reliable when the absolute correction value is less than 0.20–0.25 dex. However, it should be understood that the greater the correction, the larger its potential error due to complex dependences on microturbulent velocity, sulfur abundance, and other factors. Overall, the computed correction grid can be used to assess the degree of non-LTE effects on sulfur lines. For lines with larger non-LTE corrections, individual calculations of both b-factors and synthetic spectra are advisable.

If we compare our non-LTE calculations with those based on the 2009 atomic model (Korotin et al. 2017), the corrections for stars with near-solar metallicity are quite similar between the two models. For metal-poor stars, the new model generally shows slightly smaller departures from LTE. For instance, using the old atomic model, for the $\lambda 9212$ Å line for a star with parameters [Fe/H] = -1.0, log g = 2, and $T_{\text{eff}} = 6000$ K the correction was approximately -0.85 dex, whereas the new model yields a smaller value: -0.75 dex. For dwarfs with log g = 4, the difference is smaller: ~ 0.39 and -0.34, respectively. This is due to the use of detailed quantum-mechanical calculations of collisional rates in the new model instead of approximate formulas from model Korotin (2009). It is worth noting that there can be substantial differences between our data and calculations from Takeda et al. (2005). Specifically, for the $\lambda 9212$ Å line in a star with parameters [Fe/H] = -1.0 and $T_{\text{eff}} = 6000$ K, the calculations in Takeda et al. (2005) yield corrections of -1.02 for a giant (log g = 2) and -0.26 dex for a dwarf (log g = 4). The study Takada-Hidai & Takeda (1996) provides non-LTE correction estimates for lines of the sixth multiplet ($\lambda 8694$ Å) in A-stars with log g = 4 and T_{eff} from 8000 to 12000 K. The correction values for temperatures below 9500 K are similar to ours, but at higher temperatures, they remain negative, albeit small in magnitude.

7. CONCLUSIONS

We have proposed a grid of correction to take into account the departures from LTE in neutral sulfur lines in the visible and infrared spectral regions, including the H-range. The grid was calculated using a sulfur atomic model incorporating the most up-to-date atomic data on collisional rates with electrons and hydrogen. Inclusion of ionized sulfur levels and transitions in the atomic model has allowed us to extend the grid’s range of effective stellar photospheric temperatures up to 10000 K. The atomic model has proven its adequacy across a wide range of stellar parameters: sulfur lines in all test stars showed consistent element abundances regardless of non-LTE effects. The wavelengths and oscillator strengths for several multiplets were refined. A recommended list of S I lines for determining sulfur abundance has been compiled. The recommended sulfur line parameters represent a compromise between observed stellar spectra and theoretical calculations of wavelengths and oscillator strengths. The best option for obtaining precise line parameters would be laboratory measurements for all sulfur lines used in the analysis.

8. SUPPLEMENTARY INFORMATION

The online version contains supplementary material available at <https://doi.org/10.1134/S1063772924700987>.

References

- Allen, C. W. 1973, *Astrophysical quantities* (University of London, Athlone Press)
- Asplund, M., Amarsi, A. M., & Grevesse, N. 2021, *A&A*, 653, A141
- Barklem, P. S. & O’Mara, B. J. 1997, *MNRAS*, 290, 102
- Barklem, P. S., O’Mara, B. J., & Ross, J. E. 1998, *MNRAS*, 296, 1057
- Belyaev, A. K. & Voronov, Y. V. 2020, *ApJ*, 893, 59
- Biemont, E., Quinet, P., & Zeippen, C. J. 1993, *A&AS*, 102, 435
- Carlsson, M. 1986, *Uppsala Astronomical Observatory Reports*, 33
- Castelli, F. & Kurucz, R. L. 2003, in *Modelling of Stellar Atmospheres*, ed. N. Piskunov, W. W. Weiss, & D. F. Gray, Vol. 210, A20
- Cunto, W., Mendoza, C., Ochsenbein, F., & Zeippen, C. J. 1993, *A&A*, 275, L5
- Deb, N. C. & Hibbert, A. 2008, *Atomic Data and Nuclear Data Tables*, 94, 561
- Drawin, H.-W. 1968, *Zeitschrift für Physik*, 211, 404
- Froese Fischer, C., Tachiev, G., & Irimia, A. 2006, *Atomic Data and Nuclear Data Tables*, 92, 607

- Galazutdinov, G. A. 2022, *Astrophysical Bulletin*, 77, 519
- Hirata, R. & Horaguchi, T. 1994, *VizieR Online Data Catalog: Atomic Spectral Line List (Hirata+ 1995)*, *VizieR On-line Data Catalog: VI/69*. Originally published in: Department of Astronomy, Faculty of Science, Kyoto University, and, National Science Museum, 3-23-1 Hyakunin-cho, Shinjuku-ku, Tokyo
- Irimia, A. & Froese Fischer, C. 2005, *Phys. Scr*, 71, 172
- Israeli, G. & Rebolo, R. 2001, *ApJ*, 557, L43
- Jofré, P., Heiter, U., Soubiran, C., et al. 2015, *A&A*, 582, A81
- Kacharov, N., Koch, A., Caffau, E., & Sbordone, L. 2015, *A&A*, 577, A18
- Kobayashi, C., Karakas, A. I., & Lugaro, M. 2020, *ApJ*, 900, 179
- Korotin, S., Andrievsky, S., Caffau, E., & Bonifacio, P. 2017, in *Astronomical Society of the Pacific Conference Series*, Vol. 510, *Stars: From Collapse to Collapse*, ed. Y. Y. Balega, D. O. Kudryavtsev, I. I. Romanyuk, & I. A. Yakunin, 141
- Korotin, S. A. 2009, *Astronomy Reports*, 53, 651
- Korotin, S. A., Andrievsky, S. M., Caffau, E., Bonifacio, P., & Oliva, E. 2020, *MNRAS*, 496, 2462
- Korotin, S. A., Andrievsky, S. M., & Luck, R. E. 1999, *A&A*, 351, 168
- Kramida, A., Ralchenko, Y., & Reader, J. 2012, in *APS Meeting Abstracts*, Vol. 43, *APS Division of Atomic, Molecular and Optical Physics Meeting Abstracts*, D1.004
- Kurucz, R. L., Furenlid, I., Brault, J., & Testerman, L. 1984, *Solar flux atlas from 296 to 1300 nm (National Solar Observatory, Sunspot, New Mexico)*
- Limongi, M. & Chieffi, A. 2003, *ApJ*, 592, 404
- Lodders, K. 2021, *Space Sci. Rev.*, 217, 44
- Lyubimkov, L. S., Lambert, D. L., Rostopchin, S. I., Rachkovskaya, T. M., & Poklad, D. B. 2010, *MNRAS*, 402, 1369
- Martin, W. C., Zalubas, R., & Musgrove, A. 1990, *Journal of Physical and Chemical Reference Data*, 19, 821
- Mészáros, S., Allende Prieto, C., Edvardsson, B., et al. 2012, *AJ*, 144, 120
- Origlia, L., Oliva, E., Baffa, C., et al. 2014, in *Society of Photo-Optical Instrumentation Engineers (SPIE) Conference Series*, Vol. 9147, *Ground-based and Airborne Instrumentation for Astronomy V*, ed. S. K. Ramsay, I. S. McLean, & H. Takami, 91471E
- Petit, P., Louge, T., Théado, S., et al. 2014, *PASP*, 126, 469
- Reiners, A., Mrotzek, N., Lemke, U., Hinrichs, J., & Reinsch, K. 2016, *A&A*, 587, A65
- Romanovskaya, A. M., Ryabchikova, T. A., Pakhomov, Y. V., Korotin, S. A., & Sitnova, T. M. 2023, *MNRAS*, 526, 3386
- Ryabchikova, T., Piskunov, N., Kurucz, R. L., et al. 2015, *Phys. Scr*, 90, 054005
- Seaton, M. J. 1962, in *Atomic and Molecular Processes*, ed. D. R. Bates (New York: Academic Press)
- Spite, M., Caffau, E., Andrievsky, S. M., et al. 2011, *A&A*, 528, A9
- Steenbock, W. & Holweger, H. 1984, *A&A*, 130, 319
- Summers, H. P. & O'Mullane, M. G. 2011, in *American Institute of Physics Conference Series*, Vol. 1344, *7th International Conference on Atomic and Molecular Data and Their Applications - ICAMDATA-2010*, ed. A. Bernotas, R. Karazija, & Z. Rudzikas (AIP), 179–187
- Takada-Hidai, M. & Takeda, Y. 1996, *PASJ*, 48, 739
- Takeda, Y., Hashimoto, O., Taguchi, H., et al. 2005, *PASJ*, 57, 751
- Tayal, S. S. & Zatsarinny, O. 2010, *ApJS*, 188, 32
- Tsymbal, V., Ryabchikova, T., & Sitnova, T. 2019, in *Astronomical Society of the Pacific Conference Series*, Vol. 518, *Physics of Magnetic Stars*, ed. D. O. Kudryavtsev, I. I. Romanyuk, & I. A. Yakunin, 247–252
- Tull, R. G., MacQueen, P. J., Sneden, C., & Lambert, D. L. 1995, *PASP*, 107, 251
- van Regemorter, H. 1962, *ApJ*, 136, 906
- Zatsarinny, O. & Bartschat, K. 2006, *Journal of Physics B Atomic Molecular Physics*, 39, 2861
- Zerne, R., Caiyan, L., Berzinsh, U., & Svanberg, S. 1997, *Phys. Scr*, 56, 459